heritage

MDPI

Article

The Return of the Warrior: Combining Anthropology, Imaging Advances, and Art in Reconstructing the Face of the Early Medieval Skeleton

Ana Curić [1], Ivan Jerković [1,*], Fabio Cavalli [2], Ivana Kružić [1], Tina Bareša [1], Andrej Bašić [3], Marko Mladineo [3], Robert Jozić [4], Goran Balić [4], Duje Matetić [4], Deni Tojčić [5], Krešimir Dolić [6,7,8], Ivan Skejić [6] and Željana Bašić [1]

1 University Department of Forensic Sciences, University of Split, Ruđera Boškovića 33, 21000 Split, Croatia; anacuric1994@gmail.com (A.C.); ivana.kruzic@forenzika.unist.hr (I.K.); tina.baresa@forenzika.unist.hr (T.B.); zeljana.basic@forenzika.unist.hr (Ž.B.)
2 Research Unit of Paleoradiology and Allied Sciences, via della Pieta 2/1, Ospedale Maggiore, 34129 Trieste, Italy; fabio.cavalli@asugi.sanita.fvg.it
3 Faculty of Electrical Engineering, Mechanical Engineering and Naval Architecture, Ruđera Boškovića 32, 21000 Split, Croatia; andrej@fesb.hr (A.B.); marko.mladineo@fesb.hr (M.M.)
4 Arts Academy in Split, Zagrebačka ulica 3, 21000 Split, Croatia; rjozic@umas.hr (R.J.); gbalic@umas.hr (G.B.); dujematetic@gmail.com (D.M.)
5 Museum of Croatian Archaeological Monuments, Gunjačina 3, 21000 Split, Croatia; detojcic@gmail.com
6 Department of Diagnostic and Interventional Radiology,, University Hospital Split, Spinčićeva 1, 2100 Split, Croatia; kdolic79@gmail.com (K.D.); iskejic@kbsplit.hr (I.S.)
7 University Department of Health Studies, University of Split, Ruđera Boškovića 35, 21000 Split, Croatia
8 School of Medicine, University of Split, 21000 Split, Croatia
* Correspondence: ivan.jerkovic@forenzika.unist.hr

Citation: Curić, A.; Jerković, I.; Cavalli, F.; Kružić, I.; Bareša, T.; Bašić, A.; Mladineo, M.; Jozić, R.; Balić, G.; Matetić, D.; et al. The Return of the Warrior: Combining Anthropology, Imaging Advances, and Art in Reconstructing the Face of the Early Medieval Skeleton. *Heritage* **2024**, *7*, 3034–3047. https://doi.org/10.3390/heritage7060142

Academic Editor: Devrim Akca

Received: 27 March 2024
Revised: 16 May 2024
Accepted: 31 May 2024
Published: 4 June 2024

Abstract: Reconstructing the face from the skull is important not only for forensic identification but also as a tool that can provide insight into the appearance of individuals from past populations. It requires a multidisciplinary approach that combines anthropological knowledge, advanced imaging methods, and artistic skills. In the present study, we demonstrate this process on the skull of an early medieval warrior from Croatia. The skeletal remains were prepared and scanned using multislice computed tomography (MSCT) and examined using standard anthropological and radiological methods. The analysis revealed that the remains belonged to a 35–45-year-old male individual who had suffered severe cranial trauma, probably causing his death. From MSCT images, we reconstructed a three-dimensional (3D) model of the skull, on which we digitally positioned cylinders demarking the soft tissue thickness and created the face with a realistic texture. A 3D model of the face was then optimized, printed, and used to produce a clay model. Sculpturing techniques added skin textures and facial features with scars and trauma manifestations. Finally, after constructing a plaster model, the model was painted and refined by adding fine details like eyes and hair, and it was prepared for presentation in the form of a sculpture.

Keywords: MSCT; 3D modeling; facial reconstruction; forensic art; Medieval period; Croatia

1. Introduction

Facial reconstruction plays a significant role in forensic sciences, archeology, and anthropology [1–3]. It is a unique technique used to aid in building an "alive" face out of skeletal remains, which helps archaeologists in their attempts to demonstrate the appearance of the early man [4] and in the process of forensic identification [5]. The idea of anatomical sculpture "over the skeleton" began in Italy in the 18th century with the practice of ceroplasty, that is, the modeling of the muscles over the skeleton with wax [6]. The first to take an interest in this technique with forensic recognition purposes was the anatomist

Hermann Welker (1822–1897), who executed drawings on the presumed skulls of Raphael and Kant to overlap, respectively, the self-portrait and the funerary mask. Another German anatomist, Wilhelm His (1831–1904), reproduced the face of Johann Sebastian Bach from a cast of his skull after measuring the facial thicknesses from the corpses and then bringing them back to the skull of the great musician [7]. Incidentally, this underlines the difference in approach between Italians and Germans or between artistic yearning and reconstructive pragmatism. Arthur Kollmann (1858–1941) used his method to reconstruct the face of Dante Alighieri and, with the sculptor W. Buckley, reconstructed the face of a Paleolithic woman on a skull found in France using the facial thicknesses of hundreds of women of that same region [8]. In the 20th century, the leading representative of the craniofacial approximation was the Russian sculptor and anthropologist Mikail Mikyhalovic Gerasimov (1907–1970), who developed a method of approximation that was, unfortunately, never fully documented [9]. In the USA, despite the first reconstruction experiments dating back to the beginning of the 20th century, it has only been since 1946 with Krogman that facial approximation was performed regularly [10]. A forensic artist, Betty Pat Gatliff, and an anthropologist, Clyde Snow, worked on the first three-dimensional (3D) technique by inserting thick markers on the skull and connecting them with strips of clay to shape the final face [11]. In Europe, Richard Helmer and Richard Neave combined the Russian with the American method by creating the Manchester project: Neave placed thicker markers on craniometric points as in the American method by modeling the muscles and subcutaneous structures as in the Russian method [12]. The first computerized system was developed at University College London in the 1980s and was based on a system used for cranial reconstructions in surgery [13]. Since then, other computer systems have been developed using warping or parametric transformation techniques [14].

With the advancement of technology and new software for digital modeling, the use of clay for 3D facial sculptures is increasingly being replaced by 3D printing digitally shaped faces, which utilize computed tomography (CT) scans of the skull as their foundation. For instance, the facial reconstruction of the pharaoh Tutankhamun was entirely digital [15]. Modern technologies enabled calculations that allow computationally predicting the appearance of missing parts of the skull. This was the case in the digital facial reconstruction of the famous writer Dante Alighieri with a missing mandible [16]. The interdisciplinary example used for creating the face of King Richard III was based on the utilization of forensic digital facial reconstruction, sculpture art, and historical sources to achieve a more realistic representation [17].

In Croatia, facial reconstruction has brought to life the faces of archaeological populations and saints. The face of the mummified remains of Saint Nicolosa Bursa was revived using MCTS scans and a 3D-printed model of the skull. The Manchester method was used to place pins to measure tissue thickness at specific points on the skull, allowing the saint's face to be sculpted from clay [18]. Entirely digitally created facial reconstructions have been used to revitalize the face of an early medieval man from the Rižinice site [19], a man buried in the atrium of the pre-Romanesque church in Lobor [20], and a victim of the Second World War from Gračani [21].

The present study aimed to utilize a multidisciplinary approach combining archaeology, anthropology, radiology, 3D technologies, and art to reconstruct the face of an Early Medieval warrior from Croatia. By integrating these methods, we aimed to provide a detailed and realistic facial reconstruction that offers insights into the individual's appearance and historical context while addressing the challenges of non-destructive cultural heritage analysis.

2. Materials and Methods

2.1. Archaeological Setting

The archaeological site of Ostrovica, a Croatian early medieval site, is located 18 km from the town of Benkovac in the northern Dalmatia region. Ostrovica's strategic location, sheltered by geographical position and close to vital trade routes, has ensured its continuous settlement throughout history. In the 1980s, the first major archaeological analysis was conducted, confirming the existence of an early medieval cemetery. A total of 115 graves were discovered, revealing the presence of two separate groups. Most of the 108 graves were on the edges of the burial site, with the remaining seven graves being found further north and forming the second group. These burials can be dated to the early ninth century and are described as the oldest burial horizon, mainly consisting of single graves [22–25]. A male from Grave 63 belonged to the first burial group and was buried in a wooden coffin with no grave goods.

2.2. Anthropological Analysis

After the archaeological excavation, a total of 115 early medieval graves were uncovered and transported to the Forensic and Biological Anthropology Laboratory of [24]. For all skeletal remains, biological profiles were reconstructed and documented. Sex was assessed by examination of pelvic and cranial traits, while age was estimated by examining the auricular surface of the ilium, tooth wear, and degenerative changes of joints [26,27]. Pathological and traumatic changes were also analyzed [28,29], with particular attention to the skull [30]. The average height of the person was estimated using the maximum femoral length incorporated with formulas developed by Ruff et al. [31].

2.3. Radiographic Imaging and Analysis

A multi-slice computed tomography (MSCT) scanning of the skull was performed at the Department of Diagnostic and Interventional Radiology, University Hospital Center in Split, Croatia, on Somatom Definition AS© (Siemens Medical Solutions, Erlangen, Germany) with 120 KV 300 mA and a slice thickness 0.6 mm. The RadiAnt DICOM Viewer© (v. 2022.1, Medixant, Poznan, Poland) system was used on a medical monitor for postprocessing and visualization. A thorough trauma and pathology assessment was conducted. This evaluation included detailed measurements, differential diagnosis, and reconstruction of the trauma mechanism [32].

2.4. Digital Facial Reconstruction

Skull was reconstructed from the image dataset [33] through a multi-step process. First, dedicated software performed image preprocessing to isolate skull features within the images. This preprocessed data were then converted into a three-dimensional point cloud, capturing the skull's geometry. Finally, the point cloud was transformed into a surface mesh suitable for further analysis or export. Obtained skull mesh was imported into a 3D editing software, 3ds Max 2023© (Autodesk Media and Entertainment, Montreal, QC, Canada), where small cylinders were constructed and positioned orthogonally onto the virtual skull surface. These cylinders represented 25 anatomical landmarks [33], whose thickness was carefully chosen to match the tissue depth on the underlying bone structure. Literature data were consulted to guide the precise positioning of the ocular globes [34] and nasal points [35] and to define the width of the mouth [36]. After placing all the cylinders on the digital skull, the data were exported in .OBJ format and imported into FaceGen Modeller Core© 3.34 (Singular Inversion Inc., Toronto, ON, Canada) to further refine the approximation of facial features. The Photofit option in FaceGen Modeller was used to create a three-dimensional face similar to a face given through one or more photographs, but only to derive a realistic texture, while landmarks were used to create the face itself. The software created a 3D mesh of the reconstructed face with a realistic texture. This face was imported into 3D editing software, made partially transparent, and positioned next to the skull model. We utilized specialized tools to achieve a perfect alignment between the reconstructed face and the underlying bone structure of the skull. This was particularly important for areas such as the chin and forehead (Figure 1). The final reconstruction was saved in .OBJ format.

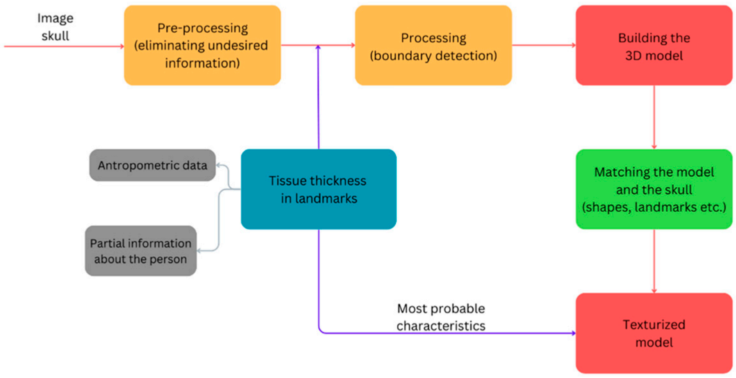

Figure 1. Facial reconstruction phases.

2.5. Optimizing and Printing a 3D Model

We imported the file in Autodesk® MeshmixerTM (v. 3.5.4.7.4., Autodesk Inc., St Rafael, CA, USA) software that we employed for postprocessing, utilizing the "Reduce" feature to decrease the number of vertices and triangles. Additionally, the "Smoother" tool was used to eliminate irregularities from specific surfaces, while the "Hollow" function was employed to reduce the model's weight and decrease printing time. To accommodate the model's size surpassing the 3D printer's capacity, it was divided into four sections utilizing Microsoft 3D Builder (v. 18.01931.0., Microsoft Corporation, Redmont, WA, USA, 2017). This software facilitated the creation, inspection, modification, and preparation of the model for 3D printing. Employing Fused Deposition Modeling (FDM) technology, the model was printed using a Prusa Mk3 i3 3D printer (Prusa, Prague, Czech Republic, 2018). We chose the material Facilan™ C8 by 3D4Makers (3D4Makers, Haarlem, The Netherlands, 2014), a biodegradable substance designed for industrial-grade 3D printing applications. Following the completion of the printing process, minimal finishing touches were necessary, involving removing support structures from the printed components and refining visible layer lines through sanding and smoothing.

2.6. Creation of Sculpture

During the facial reconstruction procedure previously generated three-dimensional computer models of the reconstruction were utilized as the starting point, along with their replicated versions produced by a 3D printer. A silicone impression was taken from the printed 3D replica of the head, which was subsequently immobilized within a two-part plaster mold. Two distinct types of silicone rubber were employed for the rubber impression extraction from the 3D print. The first type, KORAFORM K 31 A (POLYchem, Bitterfeld-Wolfen, Germany), was applied in a liquid state, allowing for precise application. The second type, BLUESIL RTV 3325 P (POLYchem, Bitterfeld-Wolfen, Germany), in a soft form, was applied through pressing, ensuring accurate replication of intricate features. After creating the silicone-plaster mold, the 3D printed model was removed, and in its place, an identical replica was crafted using the technique of casting from a modeling material, primarily clay or plasticine (in this case, clay was used). Once an adequate thickness of the new clay model had formed within the mold, it was secured with the silicone mold onto a sculpting armature for portrait modeling, designed to hold all materials in place and prevent any potential deformations or shifts of the clay core. After securing, the plaster and silicone molds were removed, and the modeling process commenced. Through this procedure, a series of mechanical traces (isohypses) formed during the 3D printing process were removed. Additionally, shaping and adjustment of the soft tissue of the earlobe were performed, and volume was added to the neck area, which was not included in the 3D-printed model. After all necessary technical modifications to the existing model were completed, the process of transforming the skin surface was initiated. Various skin textures and features around the eye, lip, and nose areas were executed to accurately represent the model's age, aligning with the analysis of the skeleton and the generated computer model. Significant traumas often result in visible damage and scars on the epidermis and soft facial tissue. Facial reconstruction enhancements were implemented through sculpting techniques, whereby effects such as scars and loose skin were incorporated. Importantly, these enhancements were applied without altering the underlying muscular and skeletal structures. Following the completion of procedures on the clay model, a plaster mold (negative) was created, from which the final plaster model (positive) was cast. A metal framework was embedded into the cast plaster model, serving simultaneously as an internal support and a sturdy base. Subsequently, the plaster model was thoroughly dried and prepared for final patination or surface painting. During the painting and patination process, a wide range of acrylic-based colors were utilized and applied onto the plaster substrate of the model in multiple translucent layers of varying intensity and tonality to achieve a more convincing skin tone effect. Upon completion of the painting process, fine details such as eye pupils, hair, and facial hair were added. Raw flax fiber was used for creating hair and facial hair details and treated with dye to achieve the desired shade. The hair and facial hair were applied to the existing model using a mixture of polyvinyl acetate and water adhesive, possessing strong penetrating properties into the plaster and flax fiber structure while remaining transparent after drying. Finally, the fully completed reconstructed head model was treated with a protective layer of clear, transparent varnish.

3. Results and Discussion

3.1. Anthropological and Radiographic Analysis

The skeleton from Grave 63 belonged to a male aged 35–45, with an estimated stature of 181.3 ± 3.21 cm. The long bones of both the upper and lower limbs were preserved, and pathological changes were visible on some bones. These changes included initial degenerative joint disease (osteoarthritis) on the proximal articular surface of the right tibia and periostitis on the diaphyses of both tibiae. Sacralization of L5 has occurred. The skull and mandible were completely preserved, except for the partly fragmented right parietal with two distinct traumas.

A large traumatic lesion was observed in the right frontotemporal parietal region (Figure 2a), characterized by a temporoparietal fracture area measuring approximately 10 cm in maximum diameter. Its upper margin extended into a horizontal fracture, involving nearly the entire frontal squama from right to left, with slight obliquity from base to top, also impacting the upper wall of the right frontal cell more cranially (Figure 2b). This complex lesion exhibited complete signs of healing (Figure 2c).

Figure 2. (**a**) CT MIP reconstruction: lines of fracture (arrows); (**b**) coronal section: signs of healing of the fracture; (**c**) fracture of the wall of the sinus frontal right cell.

Additionally, at the frontal-sphenoidal level on the same side, just above and posterior to the frontomalar suture, a puncture lesion was noted, conical with an oval base, measuring approximately 15 × 7 mm, with a trajectory from right to left and obliquely from bottom to top for 8.5 mm. (Figure 3). Cranially to this, nearly in continuation with the upper margin of the described lesion, another lesion of similar morphology, albeit smaller (5 × 2 mm) and slightly over 1 mm in depth, was observed. These lesions also appeared to have rounded margins with signs of reparative bone remodeling at their edges. Additionally, the frontomalar joint had minimal diastasis on the same side.

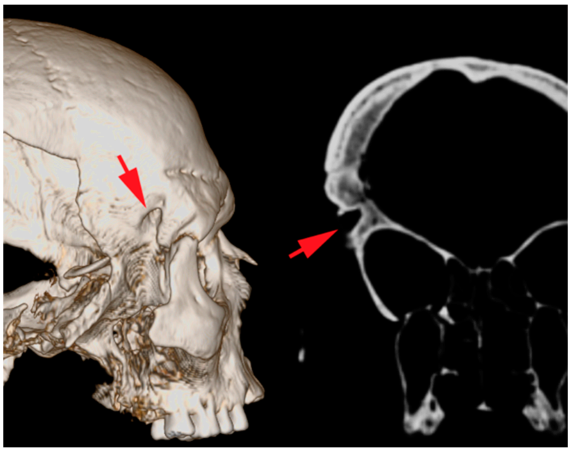

Figure 3. CT 3D reconstruction and a coronal slice of the skull: puncture lesion (arrows).

In the posterior right parietal area, there was a linear lesion with a coronal direction of approximately 46 mm, with an almost triangular cross-section, obliquely oriented relative to the tangent to the diploic surface (Figure 4). This lesion, at its medial margin, involved part of the diploic thickness and terminated in a thin linear fracture that extended to the contralateral parietal for about 52 mm.

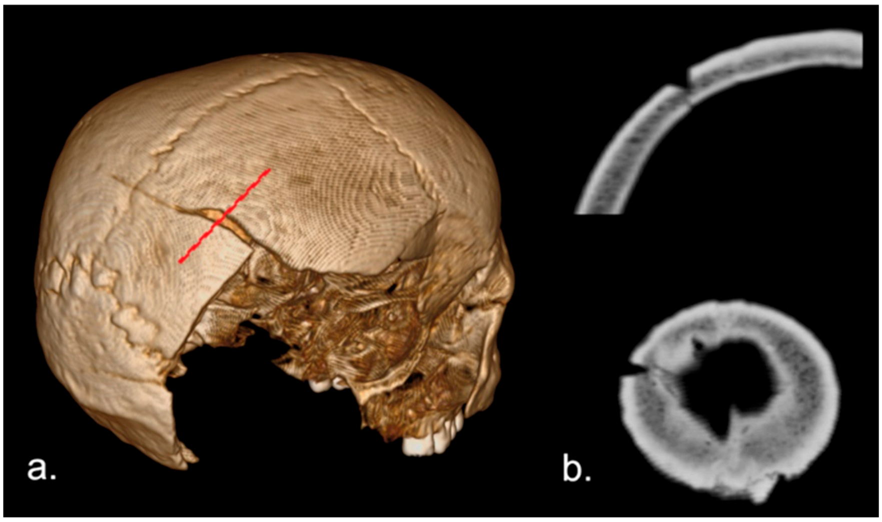

Figure 4. (**a**) CT 3D reconstruction of the skull, oblique posterior: cranial fracture line. (**b**) CT oblique slices showing the shape of the lesion.

Perpendicular to this, there was another linear, full-thickness fracture, approximately 50 mm in length, with smooth, clean fracture margins. It intersected cranially with the previous one but descended caudally to the occipital level, where it appeared to assume an "eyelet" shape, then changed direction toward the skull base. The lesion presented a thin fracture rim perpendicular to its direction, which was directed medially, affecting the squama of the occipital bone (Figure 5).

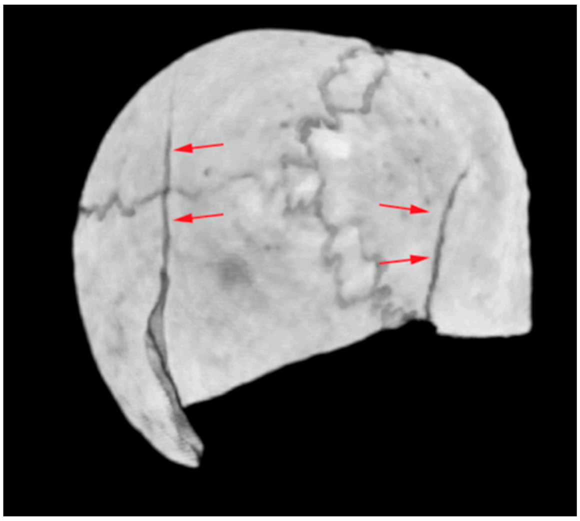

Figure 5. CT MIP skull reconstruction, posterior. Linear fractures (arrows).

Despite the well-known difficulty in classifying traumatic injuries concerning the cause and time of death [37–39], we managed to distinguish trauma types upon examination. In this case, there were two distinct events: one involving the frontotemporal parietal area, which showed almost complete signs of healing, and a traumatic event probably in two stages, evidently perimortal. In the first case, there was a wide fracture with a circular edge, connected to a fracture of the frontal squama and a rather deep "puncture lesion", which could have been caused by a complex-shaped object with a punctate surface. The fracture's morphology and the puncture lesion's direction suggest a blow from the bottom upwards, probably vibrated from behind. In the second case, it can be reasonably assumed that there were two perimortal traumatic events in sequence. Given that the two fractures intersected each other, according to the well-known "Puppe's Law" [40–42], the larger cranial fracture must have been the first, followed by the second, of greater energy. The arrangement of the terminal fractures concerning this second event is interesting, as the thin rhyme of the larger cranial fracture was evidently produced by prolonging the pre-existing, not full-thickness, fracture. The cross-section of the weapon used (assuming it was the same) and the presence of terminal fractures perpendicular to the major axis suggests the use of an axe [43,44].

3.2. Digital Facial Reconstruction

Figure 6 shows the initial phase of reconstruction of the Ostrovica male's face, which entailed positioning 25 cylinders of precise dimensions at specific points on the skull, using 3ds Max©, Autodesk. These cylinders served to delineate the thickness of tissue at each designated position.

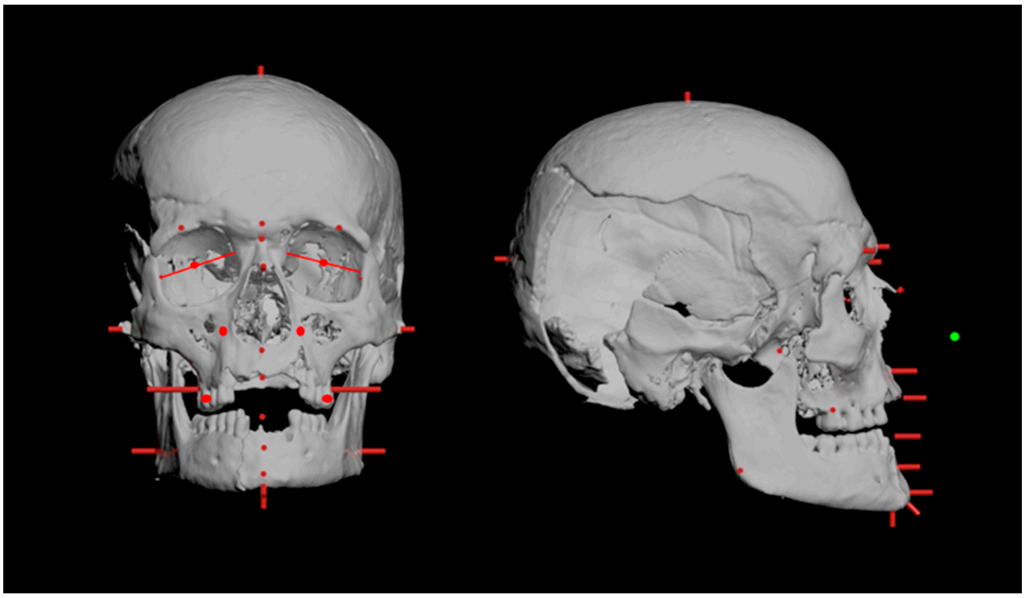

Figure 6. Positioning of the soft tissue landmarks in frontal and lateral view.

After positioning the cylinders, we integrated them with tissue thickness in the FaceGen Modeler Core v.3.34 (PhotoFit feature), and we constructed the "best facial fitting" based on landmarks. Although this software, derived from the foundational research of Vetter [45], was not initially intended for facial approximation but rather for generating diverse faces and expressions by morphing a database of average faces, it allowed for the creation of a three-dimensional face resembling a provided face from one or more photographs (frontal, right, and left profiles) by positioning predefined landmarks. Apart from landmark positioning, the photograph was solely used to derive a realistic texture, while the landmarks played a pivotal role in constructing the face itself. Additionally, the texture was chosen from the standard options available in this program.

Once all steps had been completed and the skull had been accurately positioned within the digital face model (Figure 7), the final appearance of the digital facial reconstruction was achieved (Figure 8).

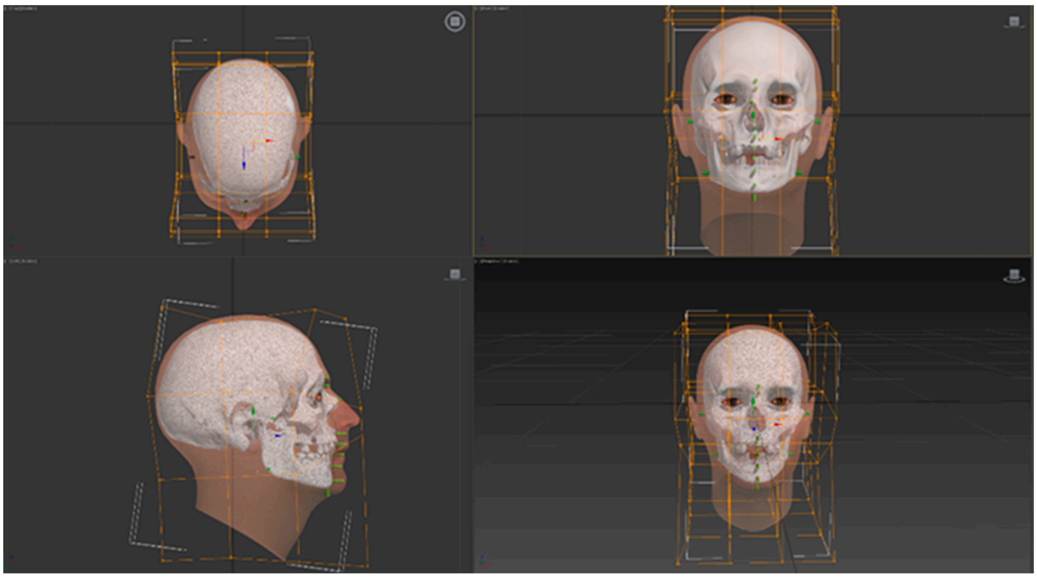

Figure 7. Matching the model and the skull.

Figure 8. Digital facial reconstruction.

3.3. Optimizing and Printing a 3D Model

The postprocessing results are shown in Figures 9 and 10, where the models' appearance after decreasing the number of vertices and triangles, as well as removing the irregularities, is visible. As previously mentioned, after weight reduction and printing time adjustment due to the printers' capacity, the model had to be divided into four segments. Table 1. shows the material consumption and price concerning the time required to print each section.

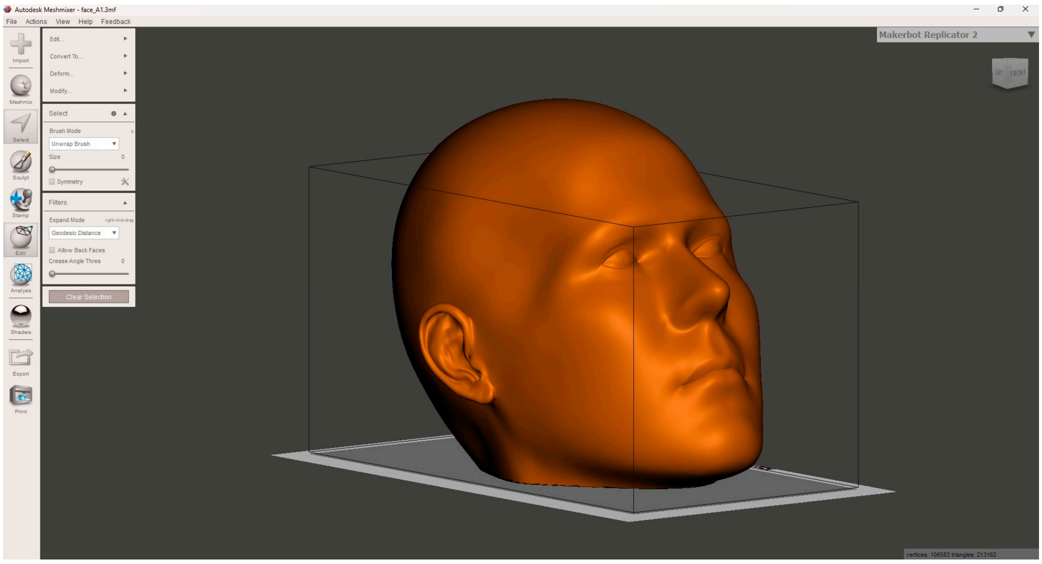

Figure 9. A cross-section of the model after using the "Hollow" function to optimize weight and printing time.

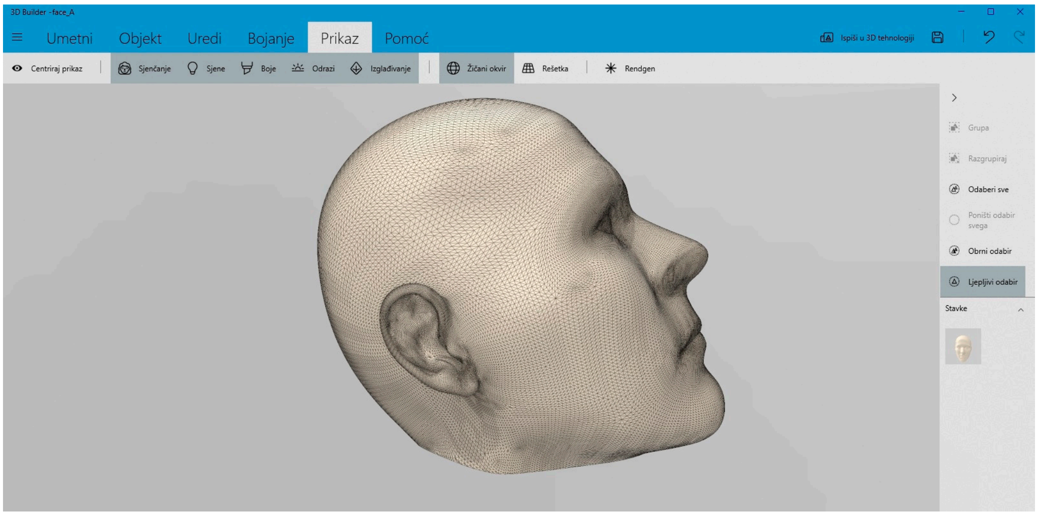

Figure 10. A virtual view of the head is rendered with a series of connected triangles (tessellation) to describe the surface geometry of the 3D design.

Table 1. Time and material consumption for 3D printing.

Section	Time (h/min)	Mass (g)	Price (€)
1. Chin area	9 h 26′	112.29	2.85
2. Mouth to ear area	8 h 20′	121.74	3.09
3. Nose end eyes area	6 h 40′	103.91	2.64
4. Skull vault area	15 h 40′	213.70	5.43
Total:	40 h 6′	551.64	14.01

After assembling the 3D-printed model, minimal finishing touches were applied, which involved removing support structures from the printed components and refining visible layer lines through sanding and smoothing. The four printed parts were finally glued to create the 3D-printed model (Figure 11).

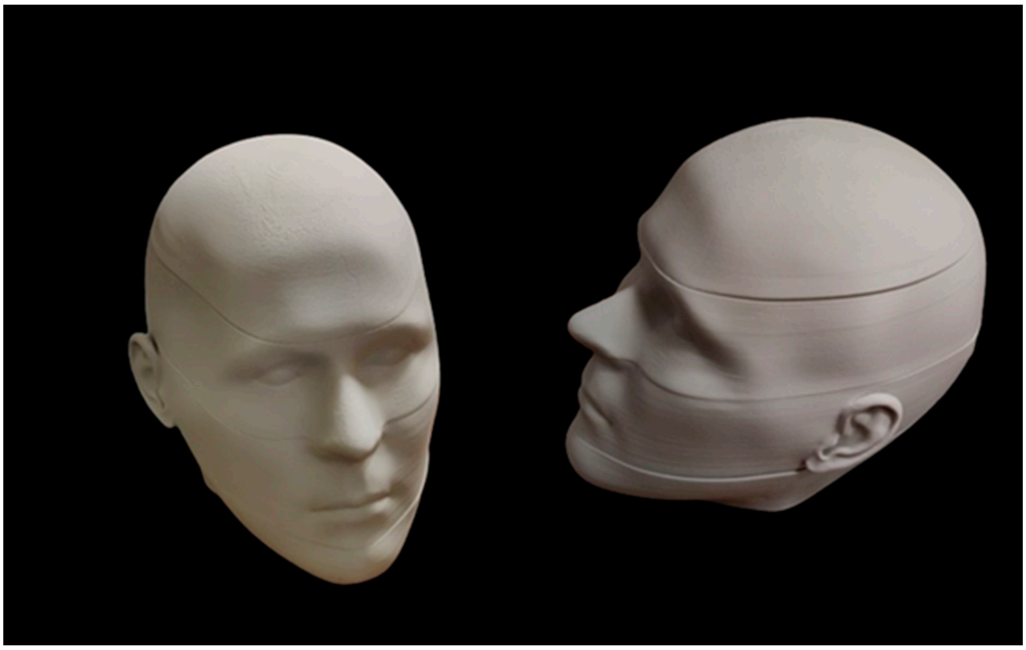

Figure 11. The figure depicts printed segments arranged to form a complete model that requires postprocessing of segment joints.

3.4. Creation of Sculpture

Figure 12a shows the first step in the making of a silicon impression of the 3D-printed model with a plaster mold, after which the face was sculpted on it using clay (Figure 12b). To enhance the modeling process and gain a more realistic bust, we added a supporting structure and neck. The ear lobes were also added at this step, which is visible in Figure 12c. The subsequent sculpting involved incorporating anthropological and radiological findings into the model. It is specifically related to a person's cranial traumas. For example, the indentation in the right frontotemporal parietal region due to severe cranial trauma likely caused the skin to hang and deform due to the lack of natural skull support, potentially affecting the area around the eyes, given that cranial injury is the second most common reason for blepharoptosis, i.e., drooping of the upper eyelid [46] (Figure 12c,d). Various acrylic colors were utilized to realistically present the skin tone (Figure 12e). Small scars were strategically added for aesthetic purposes, considering a man's estimated age (Figure 12f), to enrich the facial expression. The finishing involved adding the eyes and hair (Figure 12g), including mustaches made of raw flax fiber (cut with an unsophisticated tool for a "rustical" appearance), considering historical data about the hairstyles [47], similarly as presented in the exhibition [48]. Upon completion of the sculpture, the model was coated with a layer of clear varnish to ensure protection (Figure 12h).

Figure 12. (**a**) Making of the silicon impression with plaster molds; (**b**) start of the modeling process; (**c**) sculpting skin textures; (**d**) plaster model; (**e**) painting the skin tone on the model; (**f**,**g**) the process of adding eyes and hair; (**h**) the final product.

4. Conclusions

Here, we presented a facial reconstruction of an early medieval man, estimated to be between 35 and 45 years old. A significant aspect of the reconstruction was the incorporation of cranial traumas and their effect on facial appearance. Not only did these injuries give insight into this man's life, but they also revealed the manner of his death. The presence of both antemortem and perimortem traumas suggests a life fraught with violence or accidents, underscoring the hazards encountered by individuals in early medieval society. Consequently, this skeleton was chosen for reconstruction to be featured in an exhibition centered around warriors in Early Medieval Croatia.

After archaeologists conducted excavations and documented the discovery context of the skeletal remains, anthropologists interpreted the life of the individual reflected in the bones. Biological anthropology provided data on the person's sex, average height, age, pathological changes and identified all injuries sustained during the person's lifetime. These findings were additionally confirmed by radiologists, who examined the bones on MSCT images. This way, perimortal traumas, most probably inflicted by a sharp object, have been found and documented on the posterior right parietal area of the skull. Radiographic images were employed not only for trauma analysis but also for generating a 3D model of the skull, which was a crucial step in the process of creating a digital facial reconstruction. Tissue depth markers were placed not directly on the bone but on its digital model, avoiding damage to the skull, which is important for the non-destructive analysis of cultural heritage. Subsequently, using 3D software, the face was sculpted, and facial textures in correspondence to anthropological age estimation were added. After the adjustments between bone and digital facial reconstruction were done, the next step was 3D printing of the model. With the assistance of using 3D prints of the aforementioned digital reconstructions, artists were able to bring the face fully to life. By examining examples from modern medical documentation, scars and other changes in the skin and tissue caused by such severe cranial traumas were added. To achieve a more natural perspective, wrinkles and facial hair were added.

Considering this, the study exemplified the significance of interdisciplinary collaboration and communication in the making of facial reconstructions, especially of ancient remains. Although we reconstructed only one skull, the contribution to the field of facial reconstruction stems from the participation and integration of experts from different scientific disciplines, from initial research formulation to the exhibition of the final product. This case was specific as it did not allow for straightforward facial approximation but had many prerequirements and initial steps. The role of the forensic radiologist in the reconstruction team was crucial in the detection of trauma that was not visible macroscopically and enabled the detection of the primary cause of death of the individual. Also, the reconstructed sequence and distribution of traumas highlighted remarkable modifications in the physical appearance of this man, which, in a close collaboration of radiologists, anthropologists, and artists, featured these traumas and their consequences in the most realistic way. The final finishes, such as skin, texture, hair, and other facial details, made the reconstruction more plausible to the broader public without compromising the evidence-based findings. So, this reconstruction not only depicts the particular case but could guide more complex facial reconstructions and provide perspectives on coordinating, interpreting, and integrating multidisciplinary skills and knowledge to optimize the facial approximation results.

Author Contributions: Conceptualization, A.C., I.J., F.C., I.K., T.B., A.B., M.M., R.J., G.B., D.M., D.T., K.D., I.S. and Ž.B.; methodology, A.C., I.J., F.C., I.K., T.B., A.B., M.M., R.J., G.B., D.M., D.T., K.D., I.S. and Ž.B.; validation, A.C., I.J., F.C., I.K., T.B., A.B., M.M., R.J., G.B., D.M., D.T., K.D., I.S. and Ž.B.; anthropological analysis, A.C., I.J., I.K., T.B. and Ž.B.; radiological analysis, F.C.; virtual facial reconstruction, A.C., I.J., F.C., I.K., T.B. and Ž.B.; 3D modeling and printing, A.B. and M.M.; artistic facial reconstruction, R.J., G.B. and D.M.; data curation, A.C., I.J., F.C., I.K., T.B., A.B., M.M., R.J., G.B., D.M., D.T., K.D., I.S. and Ž.B.; writing—original draft preparation, A.C., A.B., F.C., D.M. and D.T.; writing—review and editing, A.C., I.J., F.C., I.K., T.B., A.B., M.M., R.J., G.B., D.M., D.T., K.D., I.S. and Ž.B. All authors have read and agreed to the published version of the manuscript.

Funding: This study was funded by the Croatian Science Foundation, Installation Research Project no. HRZZ-UIP-2020–02-7331—Forensic identification of human remains using MSCT image analysis (CTforID).

Data Availability Statement: Data are contained within the article.

Conflicts of Interest: The authors declare no conflicts of interest.

References

1. Stephan, C.N.; Henneberg, M. Recognition by forensic facial approximation: Case specific examples and empirical tests. *Forensic Sci. Int.* **2006**, *156*, 182–191.
2. Papagrigorakis, M.J.; Synodinos, P.N.; Antoniadis, A.; Maravelakis, E.; Toulas, P.; Nilsson, O.; Baziotopoulou-Valavani, E. Facial reconstruction of an 11-year-old female resident of 430 BC Athens. *Angle Orthod.* **2011**, *81*, 169–177.
3. Wilkinson, C.M.; Saleem, S.N.; Liu, C.Y.J.; Roughley, M. Revealing the face of Ramesses II through computed tomography, digital 3D facial reconstruction and computer-generated Imagery. *J. Archaeol. Sci.* **2023**, *160*, 105884.
4. Sertalp, E.; Moraes, C.; Bütün, E. Facial reconstruction of a deformed skull from the Roman period of Juliopolis. *Herit. Sci.* **2024**, *12*, 2.
5. Galzi, P.J.; Isaacs, H.; Der Parthogh, T. The Art of Forensics: Solving Florida's Cold Cases. Case 5 Study. *J. Forensic Sci. Crim. Investig.* **2016**, *3*, 555606.
6. Azzaroli Puccetti, M.L.; Perugi, L.; Scarani, P. Gaetano Giulio Zumbo. The founder of anatomic wax modeling. *Pathol. Annual.* **1995**, *30*, 269–281.
7. Wilkinson, C. *Forensic Facial Reconstruction*; Cambridge University Press: Cambridge, UK, 2004.
8. Wilkinson, C. Facial reconstruction—Anatomical art or artistic anatomy? *J. Anat.* **2010**, *216*, 235–250.
9. Gerasimov, M.M. *Ich Suchte Gesichter*; C. Betlesmann Verlag: Munich, Germany, 1968.
10. Krogman, W.M. The Reconstruction of the Living Head from the Skull. *FBI Law Enforc. Bull.* **1946**, *6*, 11–18.
11. Taylor, K. *Forensic Art and Illustration*; CRC Press: Boca Raton, FL, USA, 2001.
12. Prag, J.; Neave, R. *Making Faces: Using Forensic and Archaeological Evidence*; British Museum Press: London, UK, 1997.
13. Quatrehomme, G.; Cotin, S.; Subsol, G.; Delingette, H.; Garidel, Y.; Grévin, G.; Fidrich, M.; Bailet, P.; Ollier, A. A fully three-dimensional method for facial reconstruction based on deformable models. *J. Forensic Sci.* **1997**, *42*, 649–652.
14. Navic, P.; Inthasan, C.; Chaimongkhol, T.; Mahakkanukrauh, P. Facial reconstruction using 3-D computerized method: A scoping review of methods, current status, and future developments. *Leg. Med.* **2023**, *62*, 102239.
15. Moraes, C.; Habicht, M.; Galassi, F.; Varotto, E.; Beaini, T. Pharaoh Tutankhamun: A novel 3D digital facial approximation. Archivio italiano di anatomia e di embriologia. *Ital. J. Anat. Embryol.* **2023**, *127*, 13–22.
16. Benazzi, S.; Fantini, M.; De Crescenzio, F.; Mallegni, G.; Mallegni, F.; Persiani, F.; Gruppioni, G. The face of the poet Dante Alighieri reconstructed by virtual modelling and forensic anthropology techniques. *J. Archaeol. Sci.* **2009**, *36*, 278–283.
17. The Grey Friars Research Team Kennedy, M.; Foxhall, L. *The Bones of a King: Richard III Rediscovered*, 1st ed.; Thames & Hudson: New York, NY, USA, 2015.
18. Marić, J.; Bašić, Ž.; Jerković, I.; Mihanović, F.; Anđelinović, Š.; Kružić, I. Facial reconstruction of mummified remains of Christian Saint-Nicolosa Bursa. *J. Cult. Herit.* **2020**, *42*, 249–254.
19. Marić, J. Forenzična rekonstrukcija lica muškarca s lokaliteta Rižinice i aproksimacija morfologije nedostajuće mandibule. *Starohrv. Prosvj.* **2020**, *3*, 727–740.
20. Hincak, Z.; Filipec, K.; Iacumin, P.; Cavalli, F.; Mihelić, D.; Jeleč, V.; Korušić, A. Rekonstrukcija života Nepoznatog Čovjeka—Interdisciplinarni pristup. *Acta Medica Croat.* **2016**, *70*, 155–163.
21. Ćirić, I. Forenzična Rekonstrukcija Mekih Tkiva Lica Pomoću Kraniofacijalne Antropometrije i 3D Računalnih Metoda. Master's Thesis, University of Zagreb, Faculty of Humanities and Social Sciences, Zagreb, Croatia, 2019.
22. Delonga, V.; Burić, T.; Alajbeg, Z. *Arheološko-povijesna skica*; Muzej Hrvatskih Arheoloških Spomenika: Split, Croatia, 1998.
23. Bašić, Ž.; Anterić, I.; Vilović, K.; Petaros, A.; Bosnar, A.; Madžar, T.; Anđelinović, Š. Sex determination in skeletal remains from the medieval Eastern Adriatic coast–discriminant function analysis of humeri. *Croat. Med. J.* **2013**, *54*, 272–278.
24. Bečić, K. Antropološka Analiza Ranosrednjovjekovne Populacije iz Južne Hrvatske. Ph.D Dissertation, University of Split, School of Medicine, Split, Croatia, 2014.
25. Bašić, Ž.; Fox, A.R.; Anterić, I.; Jerković, I.; Polašek, O.; Anđelinović, Š.; Primorac, D. Cultural inter-population differences do not reflect biological distances: An example of interdisciplinary analysis of populations from Eastern Adriatic coast. *Croat. Med. J.* **2015**, *56*, 230–238.
26. White, T.D.; Black, M.T. *Human Osteology*, 3rd ed.; Academic Press: New York, NY, USA, 2011.
27. Iscan, M.Y.; Steyn, M. *The Human Skeleton in Forensic Medicine*; Charles C Thomas Publisher LTD: Springfield, IL, USA, 2013.
28. Aufderheide, A.C.; Rodríguez-Martín, C.; Langsjoen, O. *The Cambridge Encyclopedia of Human Paleopathology*; Cambridge University Press: Cambridge, UK, 1998.
29. Ortner, D.J. *Identification of Pathological Conditions in Human Skeletal Remains*; Academic Press: Cambridge, MA, USA, 2003.
30. Lovell, N.C. Trauma analysis in paleopathology. *Am. J. Phys. Anthropol.* **1997**, *104*, 139–170.
31. Ruff, C.B.; Holt, B.M.; Niskanen, M.; Sladék, V.; Berner, M.; Garofalo, E.; Garvin, H.M.; Hora, M.; Maijanen, H.; Niinimäki, S.; et al. Stature and body mass estimation from skeletal remains in the European Holocene. *Am. J. Phys. Anthropol.* **2012**, *148*, 601–617.
32. Heller, M.; Fink, A. (Eds.) *Radiology of Trauma*; Medical Radiology Series; Springer: Berlin/Heidelberg, Germany, 2000.
33. Stephan, C.N. The Application of the Central Limit Theorem and the Law of Large Numbers to Facial Soft Tissue Depths: T-Table Robustness and Trends since 2008. *J. Forensic Sci.* **2014**, *59*, 454–462.

34. Stephan, C.N. Facial approximation: Globe projection guideline falsified by exophthalmometry literature. *J. Forensic Sci.* **2002**, *47*, 730–735.
35. Rynn, C.; Wilkinson, C.; Peters, H.L. Prediction of nasal morphology from the skull. *Forensic Sci. Med. Pathol.* **2010**, *6*, 20–34.
36. Stephan, C. Facial approximation: An evaluation of mouth-width determination. *Am. J. Phys. Anthropol.* **2003**, *121*, 48–57.
37. Cappella, A.; Amadasi, A.; Castoldi, E.; Mazzarelli, D.; Gaudio, D.; Cattaneo, C. The difficult task of assessing perimortem and postmortem fractures on the skeleton: A blind text on 210 fractures of known origin. *J. Forensic Sci.* **2014**, *59*, 1598–1601.
38. Kranioti, E. Forensic investigation of cranial injuries due to blunt force trauma: Current best practice. *Res. Rep. Forensic Med. Sci.* **2015**, *5*, 25–37.
39. Ribeiro, P.; Jordana, X.; Scheirs, S.; Ortega-Sánchez, M.; Rodriguez-Baeza, A.; Mcglynn, H.; Galtés, I. Distinction between perimortem and postmortem fractures in human cranial bone. *Int. J. Leg. Med.* **2020**, *134*, 1765–1774.
40. Christensen, A.; Passalacqua, N.; Bartelink, E. *Forensic Anthropology: Current Methods and Practice*; Elsevier: Amsterdam, The Netherlands, 2014.
41. Puppe, G. On the priority of the skull fractures. *Med. Expert News Pap.* **1914**, *20*, 307–309.
42. Symes, S.; L'Abbé, E.; Chapman, E.; Wolff, I.; Dirkmaat, D. Interpreting traumatic injury to bone in medicolegal investigation. In *A Companion to Forensic Anthropology*; Dirkmaat, D., Ed.; Blackwell Publishing: Hoboken, NJ, USA, 2012; pp. 340–389.
43. Anderson, T. Cranial Weapon Injuries from Anglo-Saxon Dover. *Int. J. Osteoarchaeol.* **1996**, *6*, 10–14.
44. Carty, N. Evidence for Cranial Trauma and Treatment in Medieval Klidare. *J. Kidare Archaeol. Soc.* **2013**, *10*, 49–80.
45. Blanz, V.; Vetter, T. A morphable model for the synthesis of 3D faces. In Proceedings of the 26th Annual Conference on Computer Graphics and Interactive Techniques, Los Angeles, CA, USA, 8–13 August 1999; p. 187.
46. Jacobs, S.M.; Tyring, A.J.; Amadi, A.J. Traumatic Ptosis: Evaluation of Etiology, Management and Prognosis. *J. Ophthalmic Vis. Res.* **2018**, *13*, 447–452.
47. Friedman, J.B. Hair and Social Class. In *A Cultural History of Hair in the Middle Ages*; Bloomsbury Publishing: Hoboken, NJ, USA, 2020; p. 137.
48. Liebieghaus. Die Grosse Illusion: Veristische Skulpturen Und Ihre Techniken. In *Liebieghaus Skulpturensammlung*; Roller, S., Ed.; Hirmer: München, Germany, 2014.